Constrained State Feedback Speed Control of PMSM Based on Model Predictive Approach

Tomasz Tarczewski and Lech M. Grzesiak, *Senior Member, IEEE*

***Abstract*—This paper presents constrained state feedback speed control of a permanent-magnet synchronous motor (PMSM). Based on classical control theory, nonlinear state-space model of PMSM is developed. A simple linearization procedure is employed to design a linear state feedback controller (SFC). Digital redesign of a SFC is carried out to achieve discrete form suitable for implementation in a DSP. Model predictive approach is used to *a posteriori* constraint introduction into control system. It overcomes limitations of motion control system with nonconstrained SFC resulting in low dynamic properties. The novel concept utilizes machine voltage equation model to calculate the boundary values of control signals which provide permissible values of the future state variables. Secondary control objectives such as zero d-axis current are included. Simulation and experimental results are presented to validate the proposed constrained state feedback control algorithm in comparison to nonconstrained state feedback control and cascade control structure, respectively.**

***Index Terms*—Constrained control, model predictive approach, permanent-magnet synchronous motor (PMSM), state feedback controller (SFC), variable-speed drive (VSD).**

I. Introduction

PERMANENT-MAGNET synchronous motors (PMSM) are widely used in motion control applications. Due to its excellent dynamic properties and compact structure, they are commonly used in a servo-drive applications such as machine tools and industrial robots [1]. Because of its superior power density and high efficiency, a new trend is to use the converter-fed-based variable speed drives (VSD) with PMSM in automotive: as a main drive in an electrical vehicle (EV), hybrid vehicle (HEV), or as an auxiliary drive in a heating, ventilating, air conditioning (HVAC) or electric power steering (EPS) applications [2]–[5].

Speed control of VSD with PMSM is most often realized by using cascade control structure with PI controllers [6]. Sliding mode approach [7] or nonlinear control based on fuzzy logic [8] and neural networks [9] can also be used in cascade structure in order to ensure robustness of the drive. Cascade control structure depicted above includes a few PI single-loop control systems. In such a case controllers must be tuned separately in a specified order (i.e., from the inner to the outer control loop). In order to avoid ringing and large overshoots, bandwidth of cascade linear controllers is often limited. As a result, a fairly modest speed control dynamic is achieved [10].

An alternative approach to speed control of PMSM is to use state feedback controller (SFC). In this structure, only one controller for all state-space variables is designed. In spite of many advantages of this structure (i.e., guaranteed robustness and nonlinearity tolerance [11], ability to control nonlinear plant [12]), the main drawbacks are: determination of SFC coefficients, taking into account constraints of a state and control variables. The traditional tuning method for SFC coefficients is based on the trial-and-error procedure. If linear-quadratic (LQR) design method is employed, the diagonal elements of weighting matrices may be initially selected using Bryson's rule [13]. On the other hand, SFC coefficients can be determined by applying computer-aided optimization methods such as particle swarm optimization (PSO) [14] or genetic algorithm (GA) [15]. Constrained control of VSD with PMSM is not trivial due to relatively short time required for execution of control algorithm (it is in a range from 50 to 100 μs for a typical switching frequency $10 \div 20$ kHz). Because of this, complex control techniques like linear matrix inequalities (LMI) cannot be used to introduce constraints into control algorithm. Good knowledge about mathematical model of the drive [i.e., PMSM with voltage source inverter (VSI)] causes that methods based on model predictive approach can be taken into account [16]. There are two approaches to cope with the constraints [17]: 1) the control design is performed directly by taking into account constraints and 2) the constraints are added *a posteriori*, after synthesis of controller. The first criterion is more complex and it can be realized with the help of a model predictive control (MPC) [18]–[21]. In this approach, solution of optimal control problem over a finite horizon is required. Since computation effort of this method is high, an implementation requires fast processing units. For example, in [19], cascade MPC control structure for a PMSM is implemented in SIMULINK and downloaded into xPC target environment. In this solution, the inner current control loop is based on receding horizon control using the linearized model of the PMSM.

Manuscript received March 25, 2015; revised June 23, 2015 and August 28, 2015; accepted October 5, 2015. Date of publication November 3, 2015; date of current version May 10, 2016.

T. Tarczewski is with the Institute of Physics, Faculty of Physics, Astronomy and Informatics, Nicolaus Copernicus University, Toruń 87-100, Poland (e-mail: ttarczewski@fizyka.umk.pl).

L. M. Grzesiak is with the Institute of Control and Industrial Electronics, Warsaw University of Technology, Warsaw 00-662, Poland (e-mail: lech.grzesiak@ee.pw.edu.pl).

Color versions of one or more of the figures in this paper are available online at http://ieeexplore.ieee.org.

Digital Object Identifier 10.1109/TIE.2015.2497302

The outer loop is also an MPC. The sampling period is chosen as 100 μs for the inner loop and 200 μs for the outer loop. In [20], an MPC algorithm for PMSM is implemented in FPGA control board (Altera Cyclone IV FPGA). In this solution, the voltage saturation and the current limitation constraints are taken into account in order to define the most suitable reference current and voltage PWM. Thanks to fast processing unit, an accurate discrete-time model of the drive is used. The sampling period is chosen as 102.4 μs while MPC algorithm is carried out in about 2.4 μs thanks to the superior FPGA computational performance. In [21], the authors use dSPACE 1004 processor for implementation of a predictive torque control of induction machine. A state-space model of machine is updated at every sampling period and employed to predict the future current and flux values. The sampling period for the predictive control algorithm is 50 μs. The overall system performance is improved by time delay compensation. A very promising solution is presented in [10], where model predictive direct speed control (MP-DSC) of PMSM is implemented in TMS320F240 DSP. The designed controller is based on the finite control set (FCS) MPC approach. In order to keeping the switching frequency low and to reduce of the computation time, a switching state graph was introduced. Although the switching frequency is variable in the proposed solution, the authors report that the torque quality can be accepted. In the second approach (i.e., *a posteriori* constraint introduction), a two-step design process is proposed. First, the linear controller ignoring state and control variables limitations are designed. The second step is to introduce constraints to maintain state and control variables in a specified ranges. An *a posteriori* introduction of constraints into control algorithm seems to be attractive due to its low computational effort.

In this paper, the model predictive approach to constraints (MPAC) introduction into control system with PMSM and SFC is proposed. It overcomes limitations of nonconstrained SFC resulting in low dynamic properties. The SFC for speed control of PMSM is based on LQR optimization method. During designing process of SFC, a state-space representation of an augmented system (i.e., linearized model of a PMSM fed by VSI with auxiliary controller state) is utilized. Digital redesign of SFC is performed to achieve discrete form suitable for implementation in a DSP. A novel *a posteriori* constraint introduction for control system with SFC is proposed in this paper. Based on machine voltage equation model is updated at every sampling instant and used to calculate the boundary values of control signals which provide permissible values of the future state variables. Another benefit of the SFC with MPAC is a relatively low computational complexity with comparison to MPC. The implementation of the proposed algorithm is fairly easy, which is realized by TMS320F2812 DSP. Experimental results will be given to demonstrate effectiveness of the control scheme.

This paper is organized as follows. Section II develops SFC for a linearized and augmented model of a plant. Section III describes model predictive approach for *a posteriori* constraint introduction into control system. In addition, simulation results are also included in this section. Section IV gives the results from experimental implementation of the designed control algorithm on PMSM drive. Section V concludes this paper.

II. State Feedback Controller

Synthesis process of a SFC for speed control of PMSM can be realized with the help of LQR design method. During designing process, a state-space representation of an augmented system (i.e., linearized model of a plant with auxiliary controller state) is prepared first. Next, values of weighting matrices used in a quadratic cost function are determined and optimization problem is analytically solved (typically MATLAB lqr() function is used to find the solution of the Riccati equation and to obtain gain matrix of controller [22]). Finally, digital redesign of the SFC is done. Chebyshev quadrature formula which provides similar behavior for control systems with discrete and continuous controllers is utilized [23].

A state-space representation of nonlinear mathematical model in the rotating dq reference frame is as follows:

$$\frac{d\mathbf{x}(t)}{dt} = \mathbf{A}(\omega_m)\mathbf{x}(t) + \mathbf{B}\mathbf{u}(t) + \mathbf{E}d(t) \tag{1}$$

where

$$\mathbf{A}(\omega_m) = \begin{bmatrix} -\frac{R_s}{L_s} & p\omega_m & 0 \\ -p\omega_m & -\frac{R_s}{L_s} & -\frac{p\psi_f}{L_s} \\ 0 & \frac{K_t}{J_m} & -\frac{B_m}{J_m} \end{bmatrix}, \quad \mathbf{x}(t) = \begin{bmatrix} i_d(t) \\ i_q(t) \\ \omega_m(t) \end{bmatrix}$$

$$\mathbf{B} = \begin{bmatrix} \frac{K_p}{L_s} & 0 \\ 0 & \frac{K_p}{L_s} \\ 0 & 0 \end{bmatrix}, \quad \mathbf{E} = \begin{bmatrix} 0 \\ 0 \\ -\frac{1}{J_m} \end{bmatrix}$$

$$\mathbf{u}(t) = \begin{bmatrix} u_{sd}(t) \\ u_{sq}(t) \end{bmatrix}, \quad d(t) = T_l(t)$$

where i_d, i_q are current space vector components, R_s, L_s denote resistance and inductance of stator, ψ_f is permanent magnet flux linkage, p is the number of pole pairs, ω_m is angular speed of the PMSM shaft, J_m is moment of inertia, K_t is torque constant, B_m is viscous friction, T_l is unmeasured load torque, u_{sd}, u_{sq} are space vector components of inverter control voltages, K_p is gain coefficient of considered inverter. At this stage, nonlinearities and dynamics of the VSI have been neglected. It was also assumed, that for a surface mounted permanent magnet machine inductances in d-axis and q-axis are in practically equal ($L_s = L_d = L_q$).

Model of PMSM presented above contains nonlinear and cross-coupled terms in the first and in the second row of a state-space equation. A short description of a simple feedback linearization procedure is given here, more detailed information can be found in [24]. First, new variables were defined

$$u_{md}(t) = \frac{p\omega_m(t)L_s i_q(t)}{K_p} \tag{2}$$

$$u_{mq}(t) = \frac{p\omega_m(t)\left(L_s i_d(t) + \psi_f\right)}{K_p}. \tag{3}$$

Next, variable (2) is added to the first row of (1) while variable (3) is subtracted from the second row of (1). Finally, linearized model of PMSM with an inverter can be rewritten in a standard form of a state-space equation as follows:

$$\frac{d\mathbf{x}(t)}{dt} = \mathbf{A}\mathbf{x}(t) + \mathbf{B}\mathbf{u}(t) + \mathbf{E}d(t) \tag{4}$$

where

$$\mathbf{A} = \begin{bmatrix} -\frac{R_s}{L_s} & 0 & 0 \\ 0 & -\frac{R_s}{L_s} & 0 \\ 0 & \frac{K_t}{J_m} & -\frac{B_m}{J_m} \end{bmatrix}, \quad \mathbf{x}(t) = \begin{bmatrix} i_d(t) \\ i_q(t) \\ \omega_m(t) \end{bmatrix}$$

$$\mathbf{B} = \begin{bmatrix} \frac{K_p}{L_s} & 0 \\ 0 & \frac{K_p}{L_s} \\ 0 & 0 \end{bmatrix}, \mathbf{E} = \begin{bmatrix} 0 \\ 0 \\ -\frac{1}{J_m} \end{bmatrix}$$

$$\mathbf{u}(t) = \begin{bmatrix} u_{ld}(t) \\ u_{lq}(t) \end{bmatrix} = \begin{bmatrix} u_{sd}(t) + u_{md}(t) \\ u_{sq}(t) - u_{mq}(t) \end{bmatrix}, d(t) = T_l(t).$$

In order to control angular speed of the PMSM without steady-state error (in a case of step variations of the reference speed and load torque), an internal model of the reference input should be added [24], [25]. An augmented state equation, after introduction the internal input model and assumption, that load torque is omitted, takes the following form:

$$\frac{d\mathbf{x}_i(t)}{dt} = \mathbf{A}_i\mathbf{x}_i(t) + \mathbf{B}_i\mathbf{u}_i(t) + \mathbf{F}_i r_i(t) \tag{5}$$

where

$$\mathbf{A}_i = \begin{bmatrix} -\frac{R_s}{L_s} & 0 & 0 & 0 \\ 0 & -\frac{R_s}{L_s} & 0 & 0 \\ 0 & -\frac{K_t}{J_m} & -\frac{B_m}{J_m} & 0 \\ 0 & 0 & 1 & 0 \end{bmatrix}, \quad \mathbf{x}_i(t) = \begin{bmatrix} i_d(t) \\ i_q(t) \\ \omega_m(t) \\ e_\omega(t) \end{bmatrix}$$

$$\mathbf{B}_i = \begin{bmatrix} \frac{K_p}{L_s} & 0 \\ 0 & \frac{K_p}{L_s} \\ 0 & 0 \\ 0 & 0 \end{bmatrix}, \mathbf{F}_i = \begin{bmatrix} 0 \\ 0 \\ 0 \\ -1 \end{bmatrix}, \begin{matrix} \mathbf{u}_i(t) = \mathbf{u}(t) \\ r_i(t) = \omega_{m\,\mathrm{ref}}(t) \end{matrix}.$$

Introduced in an augmented state equation (5), new state variable e_ω corresponds to the integral of the angular speed error

$$e_\omega(t) = \int_0^t \left[\omega_m(\tau) - \omega_{m\,\mathrm{ref}}(\tau)\right] d\tau \tag{6}$$

where $\omega_{m\,\mathrm{ref}}$ is reference value of angular speed.

In order to design SFC for augmented state-space system (5), weighting matrices $\mathbf{Q}$ and $\mathbf{R}$ that minimize the performance index

$$J = \int_0^t \left(\mathbf{x}_i^{\mathrm{T}}(t)\mathbf{Q}\mathbf{x}_i(t) + \mathbf{u}_i^{\mathrm{T}}(t)\mathbf{R}\mathbf{u}_i(t)\right) dt \tag{7}$$

have to be determined. In this paper, the most common approach based on trial-and-error procedure was used to determine weighting matrices. The following values has been chosen:

$$\mathbf{Q} = \begin{bmatrix} 0.35 & 0 & 0 & 0 \\ 0 & 20 & 0 & 0 \\ 0 & 0 & 0.1 & 0 \\ 0 & 0 & 0 & 9000 \end{bmatrix}, \quad \mathbf{R} = \begin{bmatrix} 1 & 0 \\ 0 & 1 \end{bmatrix}. \tag{8}$$

The control law of the resulting SFC is as follows:

$$\mathbf{u}(t) = -\mathbf{K}_c\mathbf{x}_i(t) = -\mathbf{K}_{cx}\mathbf{x}(t) - \mathbf{K}_{ce\omega}e_\omega(t) \tag{9}$$

TABLE I
SELECTED PARAMETERS OF THE DRIVE

Symbol	Value	Unit	Symbol	Value	Unit
P_N	628	W	R_s	0.85	Ω
I_N	3	A	L_s	4	mH
T_{eN}	1.05	Nm	K_t	0.35	Nm/A
Ω_{mN}	366	rad/s	U_{dc}	190	V
p	3		K_p	95	
B_m	1.1×10^{-3}	Nms/rad	f_{PWM}	16	kHz
J_m	1×10^{-4}	kgm^2	T_s	62.5	µs

where $\mathbf{K}_c = [\mathbf{K}_{cx}\ \mathbf{K}_{ce\omega}]$ is gain matrix of appropriate dimension. In order to obtain gain matrix $\mathbf{K}_c$, the symmetric positive definite solution of the Riccati equation has to be found [22]. The resulting continuous SFC provides zero steady-state error of ω_m for step changes of $\omega_{m\,\mathrm{ref}}$, achieves good dynamics of angular speed control, assures good disturbance compensation, and provides control strategy with zero d-axis current.

Digital redesign of the SFC was done with the help of Chebyshev quadrature formula to achieve discrete form suitable for implementation in a DSP. Discretization method used provides similar behavior for control systems with discrete and continuous controllers [23]. Utilizing Chebyshev quadrature formula, gain matrix of the discrete SFC was calculated as follows:

$$\mathbf{K}_d = \mathbf{K}_c\left(\mathbf{A}_{cl}T_s\right)^{-1}\left(\mathbf{G}_c - \mathbf{I}_n\right) \tag{10}$$

where

$$\mathbf{A}_{cl} = \mathbf{A}_i - \mathbf{B}_i\mathbf{K}_c, \quad \mathbf{G}_c = e^{\mathbf{A}_{cl}T_s} \tag{11}$$

where T_s is the sampling period, $\mathbf{I}_n$ is identity matrix of appropriate dimension.

Discrete form of the control law (9) can be expressed by the following formula [26]:

$$\mathbf{u}(n) = -\mathbf{K}_d\mathbf{x}_i(n) = -\mathbf{K}_{dx}\mathbf{x}(n) - \mathbf{K}_{de\omega}e_\omega(n) \tag{12}$$

with

$$\mathbf{K}_d = [\mathbf{K}_{dx}\ \mathbf{K}_{de\omega}] = \begin{bmatrix} k_{dx1} & k_{dx2} & k_{dx3} & k_{de\omega1} \\ k_{dx4} & k_{dx5} & k_{dx6} & k_{de\omega2} \end{bmatrix} \tag{13}$$

where n is discrete sample time index. Presented in (12), discrete form of an additional state variable $e_\omega(n)$ was obtained by using the backward Euler integration algorithm

$$e_\omega(n) = e_\omega(n-1) + T_s\left[\omega_m(n) - \omega_{m\,\mathrm{ref}}(n)\right]. \tag{14}$$

Gain matrices of discrete SFC calculated for system (5) with parameters given in Table I and for penalty matrices (8) are as follows:

$$\mathbf{K}_{dx} = \begin{bmatrix} 0.39 & 0 & 0 \\ 0 & 0.67 & 0.09 \end{bmatrix} \quad \mathbf{K}_{de\omega} = \begin{bmatrix} 0 \\ 14.1 \end{bmatrix}. \tag{15}$$

From (15), it can be seen that: 1) there are no coupling between d-axis and q-axis (the second element in the first row and the first element in the second row are equal to zero) and 2) speed control of PMSM is realized by q-axis voltage only.

III. Model Predictive Approach to Constraint

Since mathematical model of a plant is well known, model predictive approach can be used to constraint introduction into control system (MPAC). Although there are many papers devoted to MPC of PMSM (e.g., [10] and [27]), this approach is quite complex and requires solution of optimal control problem over a finite horizon in real time or explicit precalculation of this solution (e.g., based on piecewise affine approach [28]). The more simple solution based on model predictive approach is to introduce constraints *a posteriori* into developed linear control system. This framework is based on the following two-step design process: 1) design the linear controller ignoring state and control variables limitations and 2) add constraints to maintain state and control variables in a specified ranges. It has been decided to *a posteriori* introduce constraints into designed in a previous chapter state feedback control system. The choice is driven by relatively low computational effort with comparison to typical MPC. Model predictive approach will be used to proper limitation of state variables that are important for control process.

In a case of speed control of PMSM, it is important to impose constraints on a motor currents in order to keep electromagnetic torque produced by PMSM in an acceptable range. If zero d-axis current control strategy is employed, only one state variable (i.e., q-axis current) should be limited. Moreover, vector components of control voltage should also be limited to assure linear range of modulator operation. In order to impose constraint on q-axis current, the following voltage equation will be used:

$$u_{sq}(t)K_p = L_s\frac{di_q(t)}{dt} + R_s i_q(t) + e_q(t). \tag{16}$$

The space vector component of PMSM back-EMF is given by the following formula:

$$e_q(t) = p\omega_m(t)\left(L_s i_d(t) + \psi_f\right).$$

The following discrete-time equation can be obtained from (16) by applying zero-order hold discretization with a sampling period T_s [16]:

$$u_{sq}(n)K_p = \frac{1}{\delta}i_q(n+1) - \frac{\chi}{\delta}i_q(n) + e_q(n) \tag{17}$$

where $\delta = \frac{1}{R_s}\left(1 - e^{-T_s R_s/L_s}\right)$ and $\chi = e^{-T_s R_s/L_s}$.

Based on the discrete-time model (17), the boundary values of q-axis voltage that will restrict the future values of a q-axis current $i_q(n+1)$ to permissible level are obtained as

$$u_{\text{sat up}}(n) = \left(\frac{1}{\delta}i_{qn}(n+1) + e_q(n) - \frac{\chi}{\delta}i_{qn}(n)\right) \tag{18}$$

$$u_{\text{sat down}}(n) = \left(-\frac{1}{\delta}i_{qn}(n+1) + e_q(n) - \frac{\chi}{\delta}i_{qn}(n)\right) \tag{19}$$

where $u_{\text{sat up}}(n)$ is maximum value of q-axis voltage, $u_{\text{sat down}}(n)$ is minimum value of q-axis voltage, and $i_{qn}(n+1)$ is boundary value of q-axis current.

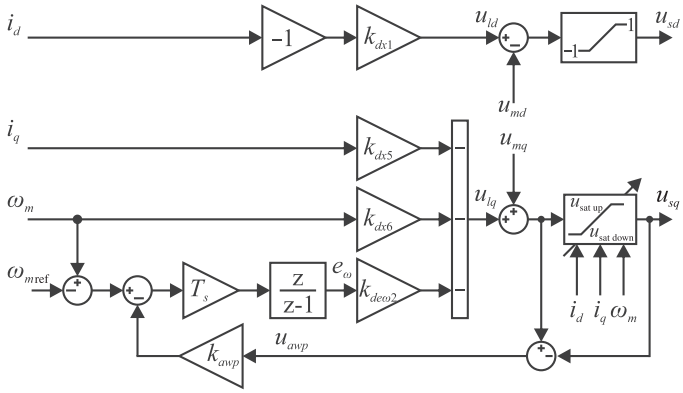

Fig. 1. Block diagram of the designed SFC with MPAC and anti-windup.

The boundary value of q-axis current usually is well-known *a priori* and remains constant. As a particular example, suppose that the boundary value of q-axis current is equal to the rated value of PMSM phase current $i_{qn}(n+1) = I_N$. On the other hand, it is possible to temporary increase the boundary value of q-axis current during start-up or in a speed reversal.

In the approach presented above, q-axis control voltage $u_{sq}(n)$ (i.e., sum of controller voltage $u_{lq}(n)$ and decoupling voltage $u_{mq}(n)$) is limited by $u_{\text{sat up}}(n)$ and $u_{\text{sat down}}(n)$ values calculated from (18) and (19) formulas in each sampling period. If the boundary values of q-axis voltage are beyond $\langle -1; 1\rangle$ range (defined by linear area of modulator operation), these are limited to ± 1, respectively. The boundary values of control signals correspond to maximum and minimum output voltages of VSI. The proposed solution provides to maintain the q-axis current in a range of $\langle -I_N; I_N\rangle$. Based on predictive equations (18) and (19), the future value of a q-axis current is limited.

Since zero d-axis current control strategy is employed to control PMSM, d-axis control voltage $u_{sd}(n)$ is only limited by linear area of modulator operation.

For a considered control system with limited control signal and SFC with internal model of reference signal (an integral path in this case), windup phenomenon may occur. In such a case, performance deterioration which causes long settling time and large overshoot can be observed [29]. To overcome this windup phenomenon, the tracking back calculation method has been adopted [30]. In this method, the difference between saturated and unsaturated control signals is used to generate a feedback signal that act on integrator input. The implementation of anti-windup path requires a change of (14) to the following form:

$$e_\omega(n) = e_\omega(n-1) + T_s\left[\omega_m(n) - \omega_{m\text{ ref}}(n) - k_{\text{awp}}u_{\text{awp}}(n)\right] \tag{20}$$

where k_{awp} devotes the antiwindup coefficient, u_{awp} is a difference between unconstrained and constrained q-axis control voltage. The value of k_{awp} was chosen empirically in order to keep the behavior of the system during saturation as close as possible to the behavior of the system without saturation. Block diagram of designed SFC with proposed MPAC and anti-windup path is shown in Fig. 1.

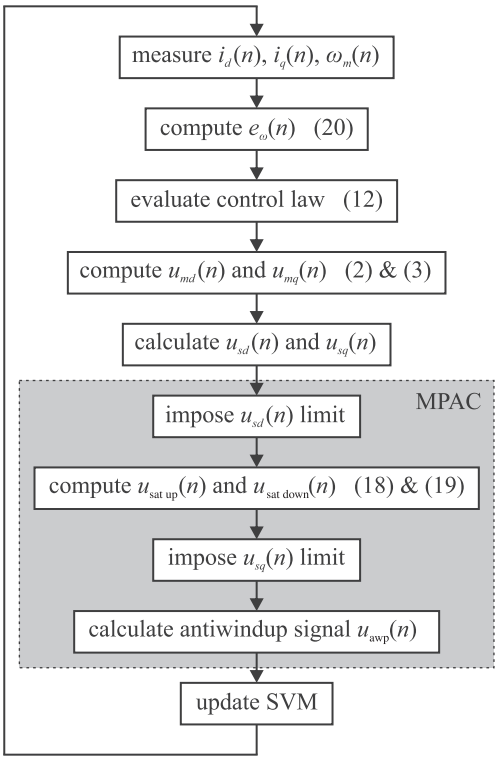

Fig. 2. Flowchart of the proposed control algorithm with MPAC.

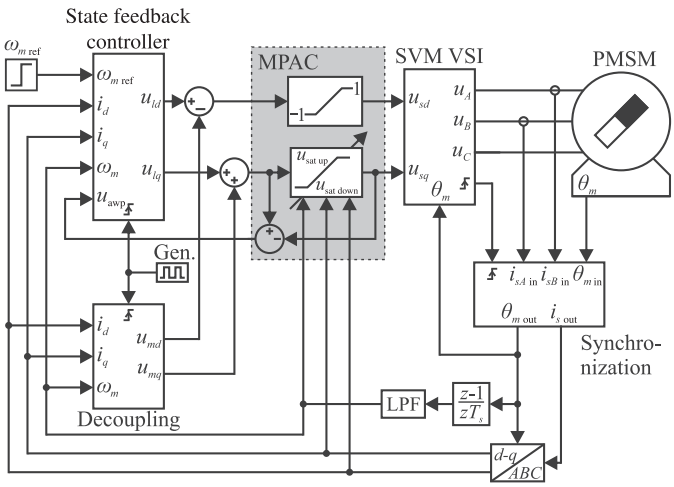

Fig. 3. Schematic block diagram of PMSM drive system with SFC and MPAC algorithm.

The flowchart of the proposed state feedback control algorithm with MPAC is shown in Fig. 2.

The general block scheme of proposed control system is presented in Fig. 3.

Simulation model of control system with proposed SFC was examined in MATLAB/Simulink environment. Designed discrete SFC was implemented in triggered subsystem to ensure proper generation of discrete control signals. An additional decoupling unit was introduced into control system in order to complement control signals u_{ld} and u_{lq} by voltages u_{md} and u_{mq}. Calculations of u_{md} and u_{mq} in decoupling unit were done according to (2) and (3), respectively. Triggered synchronization block was used to ensure that measurements are

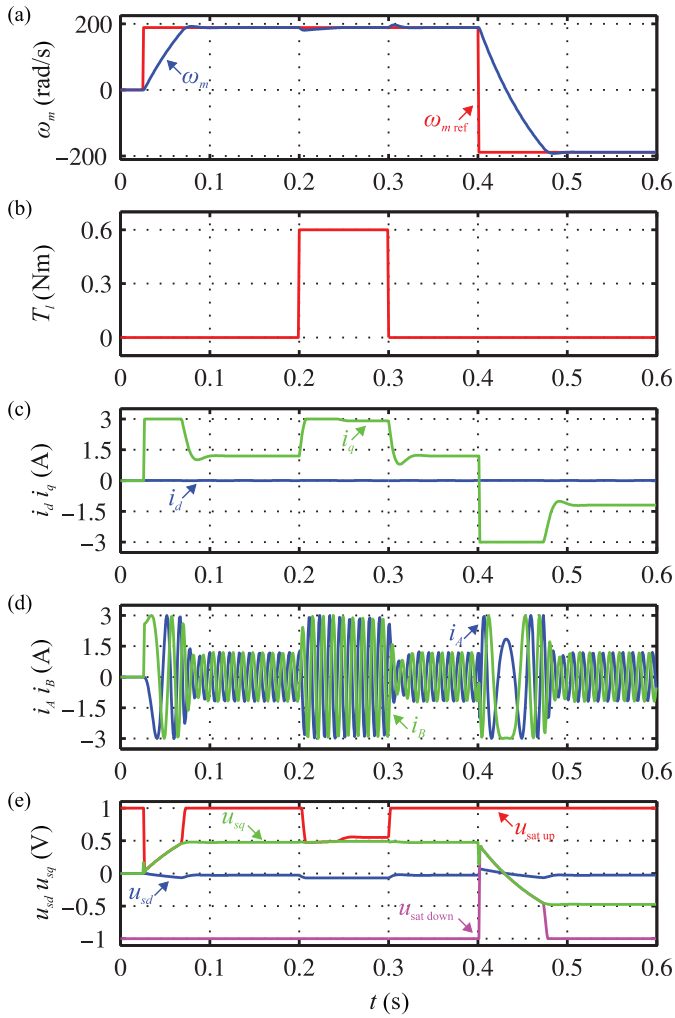

Fig. 4. Simulation response of the PMSM drive with SFC and MPAC to step changes of the reference angular velocity and load torque. (a) Speed reference and feedback. (b) Load torque reference. (c) q-axis and d-axis currents. (d) Phase currents. (e) d-q control voltages and q-axis constraints.

realized in a midpoint of the PWM pulse length. It was assumed that all state variables are measured directly and therefore in this particular case the use of estimators is not needed.

At first, the accuracy of the PMSM drive has been investigated and simulation results for SFC with MPAC are shown in Fig. 4. It can be seen from Fig. 4(c) that q-axis current of PMSM is limited properly to its rated value $i_{qn} = 3$ A during start-up. Note that during start-up value of the control voltage u_{sq} is limited by maximum value of q-axis voltage $u_{\text{sat up}}$ [Fig. 4(e)]. The speed settling time during start-up is 0.046 s. When load torque is imposed on the PMSM shaft for $t \in \langle 0.2; 0.3 \rangle$ s, the value of q-axis current increases to its rated value. An angular speed error caused by the step load is properly eliminated by proposed control algorithm. Proper q-axis current limitation (at level of $i_{qn} = -3$ A) caused by increasing value of q-axis control voltage can also be observed in speed reversal. The speed settling time in speed reversal is 0.076 s. Regardless of constraint introduction, control strategy with zero d-axis current is realized.

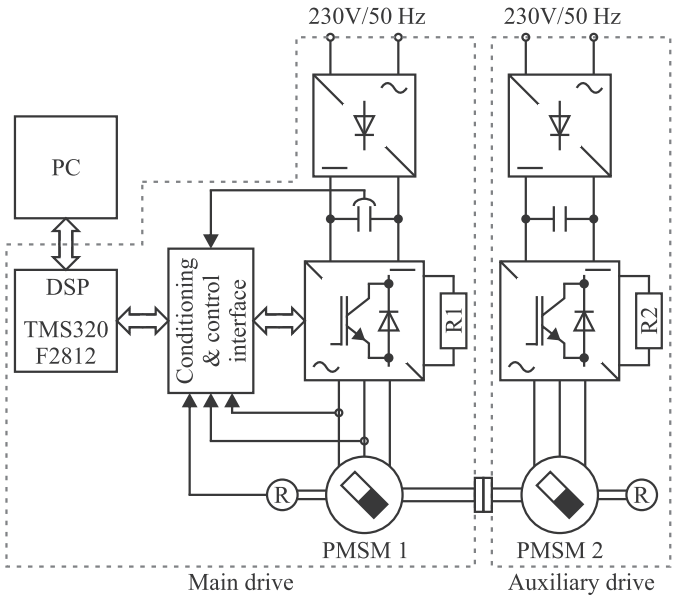

Fig. 5. Block scheme of laboratory setup.

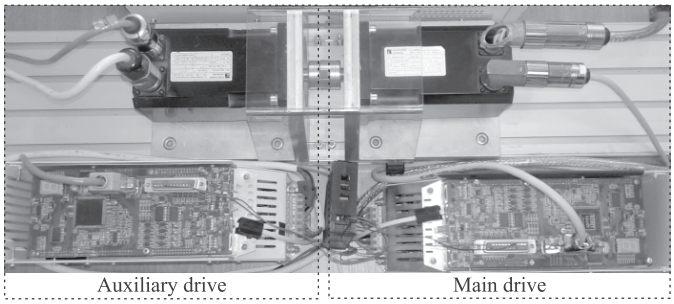

Fig. 6. Photo of laboratory setup.

IV. Experimental Results

The designed SFC with MPAC control algorithm was experimentally tested on a commercial PMSM drive. The laboratory setup (Fig. 5) consists of two identical 628 W PMSMs (Eurotherm AC M2n0150-4/1-3), each supplied by ac-dc-ac VSI (SDMT 5 made by Industrial Research Institute for Automation and Measurements in Torun, Poland) with a 16-kHz PWM switching frequency. The conditioning and control interface of considered drive system includes: resolver to digital converter (RDC), conditioning current and voltage signals from sensors to voltage in appropriate range for DSP, and IGBT drivers. The second PMSM drive operates in a torque control mode and it is used to generate load torque imposed on the primary PMSM shaft. A photo of laboratory setup is shown in Fig. 6.

Fig. 7(c) shows proper q-axis current limitation (at level of $i_{qn} = 3$ A) caused by decreasing value of q-axis control voltage [Fig. 7(e)] during start-up. The q-axis current is limited properly also in speed reversal. In this particular case, q-axis control voltage is limited by $u_{\text{sat down}}$ value. It can be seen from Fig. 7(a) that speed of PMSM is controlled without steady-state error. An angular speed error caused by the step load imposed on the PMSM shaft [Fig. 7(b)] is properly eliminated by designed control algorithm. Note that regardless of constraint introduction

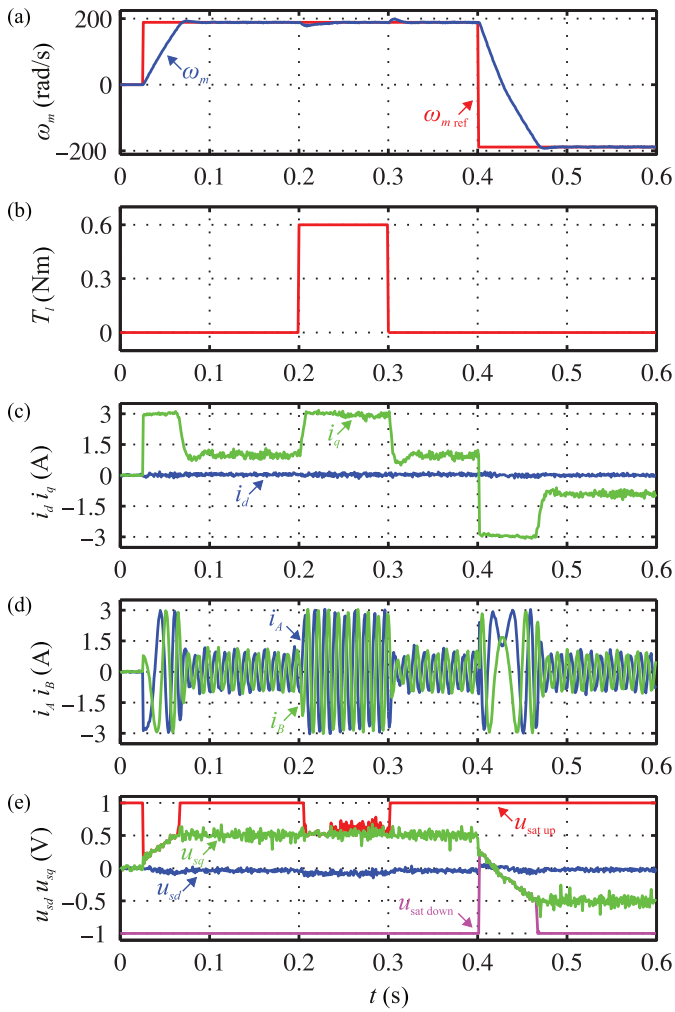

Fig. 7. Experimental response of the PMSM drive with SFC and MPAC to step changes of the reference angular velocity and load torque. (a) Speed reference and feedback. (b) Load torque reference. (c) q-axis and d-axis currents. (d) Phase currents. (e) d-q control voltages and q-axis constraints.

PMSM operates with zero d-axis current. It should be highlighted that the results of experiments (Fig. 7) are similar to simulation test results presented in Fig. 4. The speed settling time during start-up is 0.047 s while in a speed reversal is 0.075 s.

For comparative purposes, the same experimental tests were carried out for PMSM drive with nonconstrained SFC. In this case, gain matrices (8) of SFC were redesigned in order to maintain the q-axis current in a range of $\langle -I_N; I_N \rangle$

$$\mathbf{Q}_n = \begin{bmatrix} 0.35 & 0 & 0 & 0 \\ 0 & 20 & 0 & 0 \\ 0 & 0 & 0.1 & 0 \\ 0 & 0 & 0 & 57.5 \end{bmatrix} \quad \mathbf{R}_n = \begin{bmatrix} 1 & 0 \\ 0 & 1 \end{bmatrix}. \tag{21}$$

A new gain matrices of discrete SFC calculated for system (5) with parameters given in Table I and for penalty matrices (21) are as follows:

$$\mathbf{K}_{ndx} = \begin{bmatrix} 0.39 & 0 & 0 \\ 0 & 0.67 & 0.05 \end{bmatrix} \quad \mathbf{K}_{nde\omega} = \begin{bmatrix} 0 \\ 1.14 \end{bmatrix}. \tag{22}$$

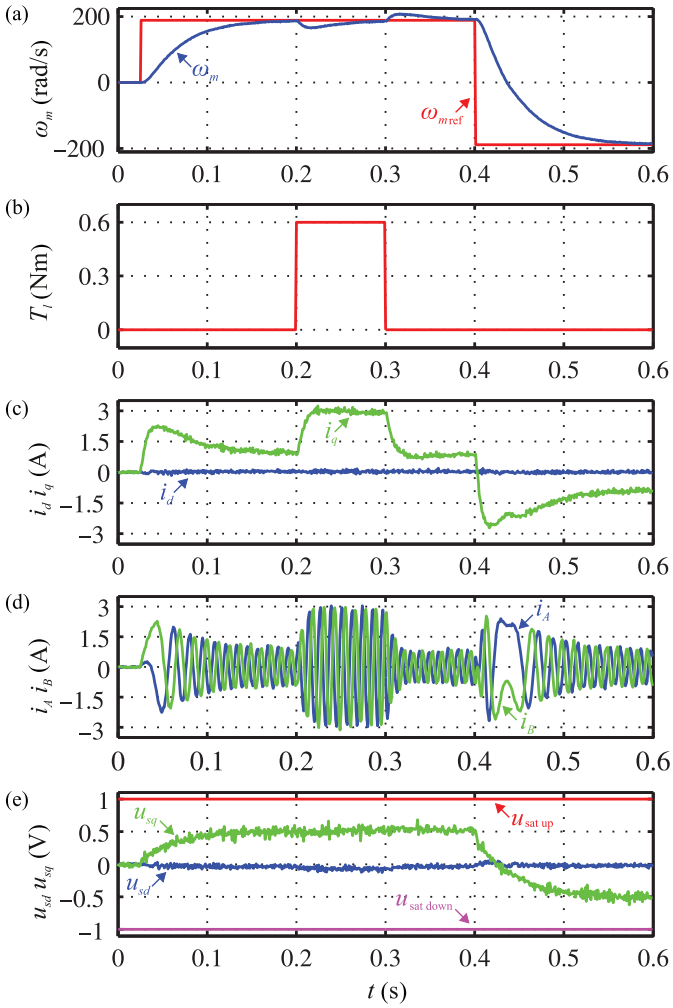

Fig. 8. Experimental response of the PMSM drive with nonconstrained SFC to step changes of the reference angular velocity and load torque. (a) Speed reference and feedback. (b) Load torque reference. (c) q-axis and d-axis currents. (d) Phase currents. (e) d-q control voltages and q-axis current.

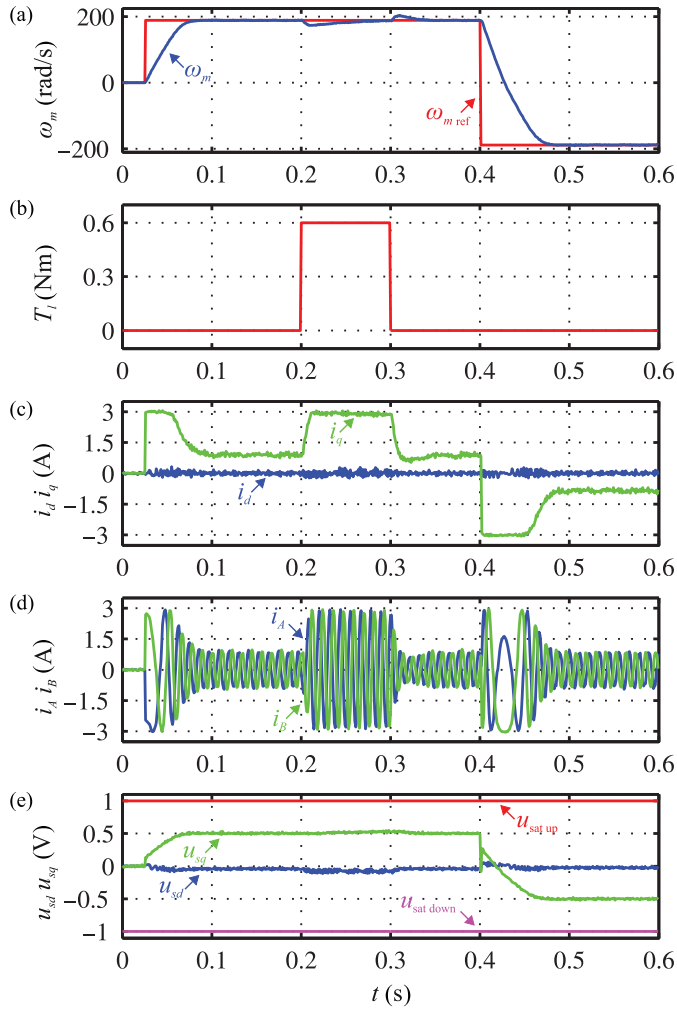

Fig. 9. Experimental response of the PMSM drive with CCS to step changes of the reference angular velocity and load torque. (a) Speed reference and feedback. (b) Load torque reference. (c) q-axis and d-axis currents. (d) Phase currents. (e) d-q control voltages and q-axis constraints.

Experimental results for PMSM drive with nonconstrained SFC are shown in Fig. 8. It can be seen from Fig. 8(c) that the value of q-axis current does not exceed its rated value but significant deterioration of a drive dynamic properties can be observed. The speed settling time during start-up is much longer (0.166 s) with comparison to result obtained for PMSM with SFC and MPAC [Fig. 7(a)]. Deterioration of a drive dynamic properties can also be observed in speed reversal—the speed settling time increases to 0.189 s. Shown in Fig. 8(e), constant values of $u_{\mathrm{sat\ up}}$ and $u_{\mathrm{sat\ down}}$ were imposed to provide operation of modulator in a linear range. It should be highlighted that better dynamic properties can be achieved if SFC with MPAC is used.

For the sake of comparison, the PMSM drive has also been designed and tested using the conventional cascade structure (CCS) with three PI controllers for the speed and current loops. An internal model (IMC) theory is utilized to design current controllers [31]. A 500 μs rise time was selected for calculate parameters of PI current controllers. This value was chosen to obtain a suitable trade-off between bandwidth and noise of current control loop. Parameters of PI speed controller were calculated with the help of symmetric-optimum criterion and retuned manually in order to reduce speed overshoot [1], [32].

Experimental test results obtained for the PMSM drive with CCS are shown in Fig. 9. Figs. 7 and 9 show the similar behavior of the SFC with MPAC and CCS during step changes of the reference angular velocity. A better load torque compensation is observed for SFC with MPAC (maximum transient speed error caused by step change of load torque at $t = 0.2$ s is 25% smaller and at $t = 0.3$ s is 30% smaller for SFC with MPAC, respectively). Enlarged part of transient speed error caused by step change of load torque is shown in Fig. 10.

Finally, dynamic properties of control schemes were examined. Small speed reference step has been applied to the drive with nonconstrained SFC, SFC with MPAC and CCS, respectively. The step was scaled in order to avoid saturation of q-axis current. Practical bandwidth was used as an indicator of the speed control performance [10]

$$f_{bw} = \frac{0.34}{t_r} \tag{23}$$

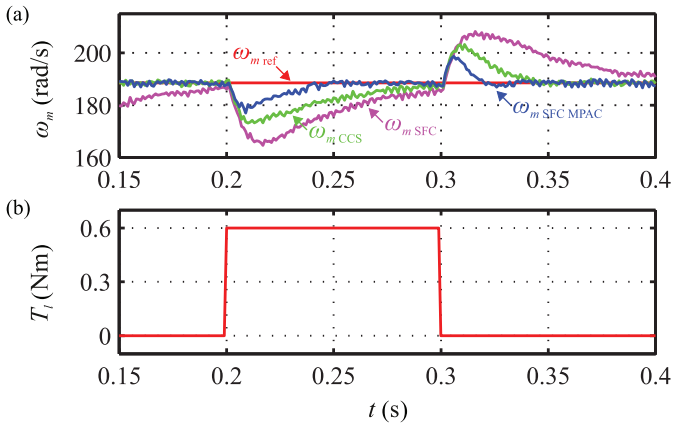

Fig. 10. Experimental response of the PMSM drive with nonconstrained SFC, SFC with MPAC and CCS to step changes of load torque. (a) Speed reference and feedback. (b) Load torque reference.

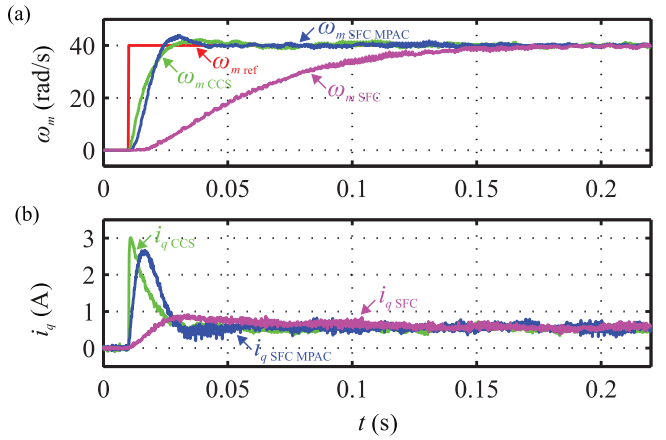

Fig. 11. Experimental response of the PMSM drive with nonconstrained SFC, SFC with MPAC and CCS to step changes of the reference angular velocity. (a) Speed reference and feedback. (b) q-axis current.

where t_r is the 10%–90% rise time. The step responses of the drive with different control algorithms have been studied and they are presented in Fig. 11. The rise times are about $t_r = 88$ ms for SFC, $t_r = 11$ ms for CCS, and $t_r = 9$ ms for SFC with MPAC, respectively. The corresponding practical bandwidths calculated from (23) are $f_{bw} = 4$ Hz for SFC, $f_{bw} = 31$ Hz for CCS, and $f_{bw} = 38$ Hz for SFC with MPAC, respectively. The application of MPAC causes that the dynamic properties of SFC and CCS are similar.

For a considered control system, the shape of PMSM acceleration is correlated with q-axis current for external load torque equal to zero. Analysis of q-axis current waveforms shown in Fig. 11(b) indicates that the more rapid changes of acceleration are occurred for CCS with PI. This disadvantage may have negative impact on mechanical parts of a driven machine.

V. Conclusion

In this paper, a novel constrained state feedback control algorithm for speed control of PMSM has been presented. Model predictive approach has been used to *a posteriori* introduce constraints into control system. The proposed solution is based on simple and accurate discrete-time model of the PMSM electrical part. Presented SFC with MPAC has shown a better performances compared to a nonconstrained SFC, particularly during start-up and in a speed reversal. Dynamic properties of the proposed control scheme are similar to cascade control structure. Moreover, it was found that the most efficient load torque compensation and the less rapid changes of PMSM acceleration are obtained for SFC with MPAC.

A relatively low computational complexity of the resulting code for constrained state feedback control is the main advantage of the proposed algorithm. Its implementation does not require fast processing unit. Presented solution can be used in a motor control applications with short time required for execution of control algorithm. Obtained simulation and experimental results confirm the potential of proposed control scheme.

References

[1] R. Krishnan, *Permanent Magnet Synchronous and Brushless DC Motor Drives*. Boca Raton, FL, USA: CRC Press, 2009.
[2] A. Sant, V. Khadkikar, W. Xiao, and H. Zeineldin, "Four-axis vector-controlled dual-rotor PMSM for plug-in electric vehicles," *IEEE Trans. Ind. Electron.*, vol. 62, no. 5, pp. 3202–3212, May 2015.
[3] F. Abrahamsen, F. Blaabjerg, and J. K. Pedersen, "Efficiency improvement of variable speed electrical drives for HVAC applications," in *Energy Efficiency Improvements in Electronic Motors and Drives*. New York, NY, USA: Springer, 2000, pp. 130–135.
[4] P. Kshirsagar, *et al.*, "Implementation and sensorless vector-control design and tuning strategy for SMPM machines in fan-type applications," *IEEE Trans. Ind. Appl.*, vol. 48, no. 6, pp. 2402–2413, Nov./Dec. 2012.
[5] Y.-C. Hung, F.-J. Lin, J.-C. Hwang, J.-K. Chang, and K.-C. Ruan, "Wavelet fuzzy neural network with asymmetric membership function controller for electric power steering system via improved differential evolution," *IEEE Trans. Power Electron.*, vol. 30, no. 4, pp. 2350–2362, Apr. 2015.
[6] I. Boldea, "Control issues in adjustable speed drives," *IEEE Ind. Electron. Mag.*, vol. 2, no. 3, pp. 32–50, Sep. 2008.
[7] J. Rivera Domínguez, A. Navarrete, M. Meza, A. Loukianov, and J. Canedo, "Digital sliding-mode sensorless control for surface-mounted PMSM," *IEEE Trans. Ind. Informat.*, vol. 10, no. 1, pp. 137–151, Feb. 2014.
[8] H. H. Choi, H. M. Yun, and Y. Kim, "Implementation of evolutionary fuzzy PID speed controller for PM synchronous motor," *IEEE Trans. Ind. Informat.*, vol. 11, no. 2, pp. 540–547, Apr. 2015.
[9] T. Pajchrowski, K. Zawirski, and K. Nowopolski, "Neural speed controller trained online by means of modified RPROP algorithm," *IEEE Trans. Ind. Informat.*, vol. 11, no. 2, pp. 560–568, Apr. 2015.
[10] M. Preindl and S. Bolognani, "Model predictive direct speed control with finite control set of PMSM drive systems," *IEEE Trans. Power Electron.*, vol. 28, no. 2, pp. 1007–1015, Feb. 2013.
[11] M. Safonov and M. Athans, "Gain and phase margin for multiloop LQG regulators," *IEEE Trans. Autom. Control*, vol. 22, no. 2, pp. 173–179, Apr. 1977.
[12] M. Brasel, "A gain-scheduled multivariable LQR controller for permanent magnet synchronous motor," in *Proc. IEEE Int. Conf. Methods Mod. Autom. Robot. (MMAR)*, 2014, pp. 722–725.
[13] G. F. Franklin, J. D. Powell, and M. L. Workman, *Digital Control of Dynamic Systems. Reading*, MA, USA: Addison-Wesley, 1998.
[14] B. Ufnalski, A. Kaszewski, and L. M. Grzesiak, "Particle swarm optimization of the multioscillatory LQR for a three-phase four-wire voltage-source inverter with an LC output filter," *IEEE Trans. Ind. Electron.*, vol. 62, no. 1, pp. 484–493, Jan. 2015.
[15] I. Robandi, K. Nishimori, R. Nishimura, and N. Ishihara, "Optimal feedback control design using genetic algorithm in multimachine power system," *Int. J. Elect. Power & Energy Syst.*, vol. 23, no. 4, pp. 263–271, May 2001.
[16] P. Cortes, M. Kazmierkowski, R. Kennel, D. Quevedo, and J. Rodriguez, "Predictive control in power electronics and drives," *IEEE Trans. Ind. Electron.*, vol. 55, no. 12, pp. 4312–4324, Dec. 2008.

[17] F. Blanchini and S. Miani, *Set-Theoretic Methods in Control*. New York, NY, USA: Springer, 2007.
[18] A. Formentini, A. Trentin, M. Marchesoni, P. Zanchetta, and P. Wheeler, "Speed finite control set model predictive control of a PMSM fed by matrix converter," *IEEE Trans. Ind. Electron.*, vol. 62, no. 11, pp. 6786–6796, Nov. 2015.
[19] S. Chai, L. Wang, and E. Rogers, "A cascade MPC control structure for a PMSM with speed ripple minimization," *IEEE Trans. Ind. Electron.*, vol. 60, no. 8, pp. 2978–2987, Aug. 2013.
[20] A. Damiano, G. Gatto, I. Marongiu, A. Perfetto, and A. Serpi, "Operating constraints management of a surface-mounted pm synchronous machine by means of an FPGA-based model predictive control algorithm," *IEEE Trans. Ind. Informat.*, vol. 10, no. 1, pp. 243–255, Feb. 2014.
[21] H. Miranda, P. Cortes, J. Yuz, and J. Rodriguez, "Predictive torque control of induction machines based on state-space models," *IEEE Trans. Ind. Electron.*, vol. 56, no. 6, pp. 1916–1924, Jun. 2009.
[22] F. Borrelli and T. Keviczky, "Distributed LQR design for identical dynamically decoupled systems," *IEEE Trans. Autom. Control*, vol. 53, no. 8, pp. 1901–1912, Sep. 2008.
[23] L. S. Shieh, W. M. Wang, and M. K. A. Panicker, "Design of PAM and PWM digital controllers for cascaded analog systems," *ISA Trans.*, vol. 37, no. 3, pp. 201–213, Jul. 1998.
[24] L. M. Grzesiak and T. Tarczewski, "PMSM servo-drive control system with a state feedback and a load torque feedforward compensation," *COMPEL*, vol. 32, no. 1, pp. 364–382, Jan. 2013.
[25] K. Ogata, *Electric Motor Drives: Modeling, Analysis, and Control*. Englewood Cliffs, NJ, USA: Prentice-Hall, 2001.
[26] L. M. Grzesiak and T. Tarczewski, "Permanent magnet synchronous motor discrete linear quadratic speed controller," in *Proc. IEEE Int. Symp. Ind. Electron. (ISIE) Conf.*, 2011, pp. 667–672.
[27] C.-K. Lin, T.-H. Liu, J. te Yu, L.-C. Fu, and C.-F. Hsiao, "Model-free predictive current control for interior permanent-magnet synchronous motor drives based on current difference detection technique," *IEEE Trans. Ind. Electron.*, vol. 61, no. 2, pp. 667–681, Feb. 2014.
[28] A. Bemporad, M. Morari, V. Dua, and E. N. Pistikopoulos, "The explicit linear quadratic regulator for constrained systems," *Automatica*, vol. 38, no. 1, pp. 3–20, Jan. 2002.
[29] S. Tarbouriech and M. Turner, "Anti-windup design: An overview of some recent advances and open problems," *IET Control Theory Appl.*, vol. 3, no. 1, pp. 1–19, Jan. 2009.
[30] H.-B. Shin and J.-G. Park, "Anti-windup PID controller with integral state predictor for variable-speed motor drives," *IEEE Trans. Ind. Electron.*, vol. 59, no. 3, pp. 1509–1516, Mar. 2012.
[31] L. Harnefors and H.-P. Nee, "Model-based current control of AC machines using the internal model control method," *IEEE Trans. Ind. Appl.*, vol. 34, no. 1, pp. 133–141, Jan./Feb. 1998.
[32] J. Umland and M. Safiuddin, "Magnitude and symmetric optimum criterion for the design of linear control systems: What is it and how does it compare with the others?" *IEEE Trans. Ind. Appl.*, vol. 26, no. 3, pp. 489–497, May/Jun. 1990.

Tomasz Tarczewski was born in Inowrocław, Poland, in 1980. He received the M.Sc. degree from Poznań University of Technology (PUT), Poznań, Poland, and the Ph.D. degree from Warsaw University of Technology (WUT), Warsaw, Poland, in 2005 and 2010, respectively, both in automatics and robotics.

Since 2010, he has been an Assistant Professor with the Institute of Physics, Nicolaus Copernicus University (NCU), Toruń, Poland, where he is a member of the research group within the Department of Technical and Applied Physics. His research interests include automatic control in drives and power electronics, with emphasis on optimal, predictive, and nonlinear control algorithms for these systems.

Lech M. Grzesiak (SM'03) received the M.Sc., Ph.D., and D.Sc. degrees in electrical engineering from Warsaw University of Technology (WUT), Warsaw, Poland, in 1976, 1985, and 2002, respectively.

In 1977, he joined WUT, where he is currently a Full Professor and holds the position of Dean of the Electrical Faculty. He has directed more than 30 R&D projects in the field of industrial electronics. He is the author or coauthor of more than 100 papers. He is the holder of more than 40 patents. His research interests include applications of artificial intelligence in control systems, generally dedicated to adjustable-speed drives, servo drives, power electronic converters, and electrical energy generating systems.

Prof. Grzesiak is an Associate Editor of the IEEE TRANSACTIONS ON INDUSTRIAL INFORMATICS.